Available online at www.sciencedirect.com

ScienceDirect

Advances in Space Research xxx (2017) xxx–xxx

ADVANCES IN SPACE RESEARCH (a COSPAR publication)

www.elsevier.com/locate/asr

Constrained optimal multi-phase lunar landing trajectory with minimum fuel consumption

S. Mathavaraj [a,1], R. Pandiyan [b,2], R. Padhi [c,*]

[a] Flight Dynamics Group, ISRO Satellite Center, Bangalore, India
[b] Dept. of Aerospace Eng., Indian Institute of Technology Madras, Chennai, India
[c] Dept. of Aerospace Eng., Indian Institute of Science, Bangalore, India

Received 21 May 2017; received in revised form 6 September 2017; accepted 10 September 2017

Abstract

A Legendre pseudo spectral philosophy based multi-phase constrained fuel-optimal trajectory design approach is presented in this paper. The objective here is to find an optimal approach to successfully guide a lunar lander from perilune (18 km altitude) of a transfer orbit to a height of 100 m over a specific landing site. After attaining 100 m altitude, there is a mission critical re-targeting phase, which has very different objective (but is not critical for fuel optimization) and hence is not considered in this paper. The proposed approach takes into account various *mission constraints* in different phases from perilune to the landing site. These constraints include phase-1 ('braking with rough navigation') from 18 km altitude to 7 km altitude where navigation accuracy is poor, phase-2 ('attitude hold') to hold the lander attitude for 35 sec for vision camera processing for obtaining navigation error, and phase-3 ('braking with precise navigation') from end of phase-2 to 100 m altitude over the landing site, where navigation accuracy is good (due to vision camera navigation inputs). At the end of phase-1, there are constraints on position and attitude. In Phase-2, the attitude must be held throughout. At the end of phase-3, the constraints include accuracy in position, velocity as well as attitude orientation. The proposed optimal trajectory technique satisfies the mission constraints in each phase and provides an overall fuel-minimizing guidance command history.

Keywords: Lunar soft landing; Constrained optimal control; Pseudo-spectral method

1. Introduction

Because of its proximity to earth, moon is often favored as a base for conducting new demonstrations in space technology. Moreover, exploration of moon has attracted the global attention since it is found to be mineral rich and also can serve as a base for solar power harvesting (Hickman et al., 1990). Further, it can also act as a base for launching ambitious missions to reach halo orbits around a Lagrangian point and to extending human explorations to interplanetary destinations (Dunham et al., 2013). In addition, proof of existence of water on moon confirmed by the impact probe of Chandrayaan-1 (Pieters et al., 2009) has given enormous hope for assistance when an envisaged lunar research base is constructed on the surface of the moon. Hence, there is a renewed interest across the globe for thorough exploration of moon.

Even though human missions have been carried out in the past for technology demonstrations, a more meaningful prolonged and cost-effective exploration of moon can hap-

* Corresponding author.
E-mail addresses: mathan@isac.gov.in (S. Mathavaraj), pandiyaraman@yahoo.com (R. Pandiyan), padhi@aero.iisc.ernet.in (R. Padhi).
[1] Also PhD Student, Dept. of Aerospace Eng., Indian Institute of Science, Bangalore, India.
[2] Also Former Group Director of Flight Dynamics Group, ISRO Satellite Center, Bangalore, India.

https://doi.org/10.1016/j.asr.2017.09.016
0273-1177/

pen only when the mission is carried out in autonomous mode with a lander-rover combination. A critical difficulty of such an autonomous mission, however, is the fact that the lander carrying the rover must soft land on the moon surface with the help of on-board sensors, processors and actuators without any human intervention. In order to meet the mission goals and precise landing sequence, the lunar landing trajectory has built-in terminal constraints at various points which must be satisfied. Landing missions on celestial bodies without atmosphere (such as moon) also demand careful planning and execution of engine burns, which minimizes the fuel consumption. If not optimized, this extra fuel must be carried in the spacecraft leading to lesser useful payload mass, and therefore, it is imperative that such a mission must be executed with minimum fuel requirement. This planning makes the overall mission quite cost effective.

Many researchers in the past have attempted to land a probe on the moon and their results have become basis for some of the decisions in descending trajectory design. It is opt to provide their research contributions: An implicit guidance logic for soft lunar landing has been attempted (McInnes and Radice, 1996) in which the lander tries to reach the designated landing point by riding on the line of sight and gradually reducing the approach velocity. However, such an intuitive and simplistic strategy normally does not lead to a proper orientation of the vehicle at the landing site. More importantly, it does not lead to a fuel optimal trajectory. Based on optimal control theory, a generic explicit guidance law has been proposed using linearized dynamics that minimizes the final time as well as the total acceleration in all three directions, thereby leading to a fuel optimal solution (DSouza, 1997). Moreover, the terminal boundary conditions on position and velocity imposed as hard constraints ensure that these constraints are met in an efficient way. Additionally, it leads to a closed form analytic formula for the necessary acceleration in both lateral and axial directions, which leads to ease of onboard implementation. Because of these characteristics, the method has attracted many researchers across the globe to use this approach to address vertical orientation of the lander while touchdown.

The desired lander orientation demands terminal acceleration which has to be enforced as a hard constraint in all three directions. The idea of including the acceleration as one of the state for addressing this constraint has been analyzed by (Uchiyama et al., 2005; Mathavaraj and Padhi, 2017). Even though, the proposed analytical guidance logic ensured vertical orientation of the lander it resulted in dynamic controller. An analytical guidance law is proposed by approximating the cost function using the trigonometric series to address the vertical landing constraint (Afshari et al., 2009). The basic formulation has been subsequently revised to account for the crew visibility and sensor capability (Lee, 2011). This approach resulted in the guidance law in which final orientation angle depends on the initial condition of the lander. So to ensure demanded orientation, a set of initial conditions has to be achieved, which may not be feasible since maneuver error results in trajectory dispersions. A summary of all these developments around the explicit guidance law originally proposed in (DSouza, 1997) can be found in a good review paper (Guo et al., 2011). An augmentation is proposed in the objective function as soft constraint to address the requirement of lander's terminal vertical orientation. Here, the aim is to minimize not only the energy but also the terminal error between the acceleration achieved and acceleration specified by the designer (Ramkiran et al., 2016).

When guidance law derived from linearized dynamics is implemented for the nonlinear system, the trajectory generated results in performance degradation. So researches are interested in finding the non-linear analytic guidance law for addressing moon landing problem. The idea is to approximate the position and velocity trajectory by a polynomial function of time. The coefficients of this polynomial are obtained using the boundary conditions. Using the non-linear dynamics the explicit guidance law is derived, which results in trajectory satisfying position, velocity, attitude boundary conditions (Sachan and Padhi, 2016). Though this technique enforces the boundary conditions, the minimum fuel consumption criterion is not addressed by this approach. Addressing the fuel consumption through the inverse polynomial guidance approach have been proposed that converts the landing problem into static optimization problem (Banerjee and Padhi, 2015). The coefficients of the guidance law are found by solving this problem using non-linear programming approach. However, owing to the usage of simplified linearized dynamics and polynomial approximation of the trajectory in the process of mathematical derivation, the explicit solution and its variants, even though appear to be elegant, do not lead to true optimal solution in general. More importantly, path and hardware constraints (which are typically necessary for a real mission) have not been imposed and hence the solution is not truly elegant.

One way of including this path constraint in optimal control formulation is by using direct trajectory optimization method. Once the guidance history satisfying all the mission constraints are obtained in ground, it is stored on onboard and followed. In literature, lunar landing problem is solved by control parameterization technique and time scaling transform (Zhou et al., 2010), which results in nonlinear guidance law addressing soft landing and terminal attitude constraint. Also, the effect of choosing the de-orbiting altitude on the landing site selection have been reported (Park and Tahk, 2011). Though the proposed method addressed path constraints it is not suited for solving the multi phase lunar landing problem. The idea of splitting the trajectory into de-orbit, braking and vertical descent for addressing terminal landing accuracy and solving this problem using Legendre pseudo-spectral technique (discussed in detail in Appendix A) has been handled earlier (Hawkins et al., 2006). However, mission constraints

Please cite this article in press as: Mathavaraj, S., et al. Constrained optimal multi-phase lunar landing trajectory with minimum fuel consumption. Adv. Space Res. (2017), https://doi.org/10.1016/j.asr.2017.09.016

resulting from landing site selection and camera look angle have not been addressed in that study. The first and second authors of this paper along with different co-worker have solved the powered descent phase of moon landing problem using Legendre pseudo-spectral and Newton method (Mathavaraj et al., 2012). This paper compared the advantages of direct and indirect optimization methods. However, the landing problem was solved as a 'single phase problem' considering only a limited number of mission constraints.

Major technological objectives of a realistic soft landing in a lunar mission however are (i) to assure precise landing, (ii) a soft touch down and (iii) selection of a favorable target site for landing (with minimum hazard). The inclusion of these objectives divides the single powered descent phase into a multi-phase problem. For example, the 'attitude hold phase' is made necessary to ensure the appropriate landing site arrival and if not, course correct to reach the landing site suitably. This phase has necessitated that guidance command generating algorithm should also account for proper attitude look angle for the on-board vision camera. However, image processing of on-board camera requires finite processing time, which demands an attitude-hold phase. This in turn imposes a constraint on the time that must be attributed to the attitude hold phase so that the image processing algorithm can give a meaningful solution. All these requirements demand a multi-phase formulation. Inclusion of this additional constraint along with soft landing constraint, the powered descent phase is split into three phases and solved in a two-dimensional framework and presented in an international conference (Mathavaraj et al., 2016). Following similar philosophy, in this paper the solution is upgraded to the three-dimensional framework along with necessary mission constraints in each phase (which include additional constraints to ensure zero velocity and attitude deviations in cross plane). Monte-Carlo analysis of optimal solution has been carried out to get an estimate of error ellipsoid. Robustness of the Legendre Pseudospectral technique is validated by envisioning to reach the same safe landing site for all the lander initial conditions taken from this error ellipsoid. It has been shown that the pseudo spectral method is quite efficient (Ross and Karpenko, 2012) and even in a multi-phase trajectory setting, the spectral method is found to be efficient as well and satisfies the terminal conditions accurately.

The rest of the paper is organized as follows. In Section 2, a point mass based governing equations in spherical coordinates and a detailed formulation of converting multi-phase problem into non-linear programming problem have been presented. This non-linear programming problem is solved for nominal condition and using this solution, error ellipsoid study is carried out for dispersed initial conditions. The guidance history in 'braking with precise navigation phase' is generated again to study the effect of these dispersion on fuel consumption. Simulation results and the mission constraints selected have been presented in detail in Section 3. Finally, conclusions of the work is consolidated and presented in Section 4. In Appendix A, a generic theory of Legendre pseudo-spectral method is provided.

2. Multi-phase problem formulation for lunar soft landing

To initiate descent trajectory, first the spacecraft is to be de-boosted from the circular parking orbit of 100 km to 18 km altitude (which is selected based on lunar terrain considerations) using a Hohmann transfer orbit. At the perilune height of 18 km, the lander is to enter into the powered descent phase. Near this phase, the propulsive engines are turned on and the lander velocity is decreased in a controlled way, to enable it to soft land on the lunar surface.

2.1. Phases in moon landing

There are three distinct phases evolved that need to be realized in order to land the lunar module on to the surface of moon. They are: (i) De-orbit maneuver phase (ii) Transfer orbit phase or coasting phase and (iii) Powered descent phase. The parking orbit of the lunar spacecraft is selected as 100 km altitude for this study. Otherwise, the method developed is general in nature and can be applied to any other orbit as well.

Deorbit phase is to maneuver the lander from 100 km parking orbit to reach 18 km altitude using Hohmann transfer principles. The lander is designed to coast to 18 km in transfer orbit phase, with appropriate conditions for the lander to approach landing site when decelerated. This is carefully planned such that retargeting and out-of-plane maneuver that costs additional fuel consumption is avoided.

Powered descent phase is initiated from the terminal conditions of the coasting phase. This phase is further split into three phases to account for various mission constraints like camera look angle, image processing time and re-targeting to a safe landing site as shown in Fig. 1. In this paper, powered descent phase is analyzed assuming that both deorbit maneuver phase and transfer orbit phase is carried out such that initial conditions for powered descent phase is planned as desired.

2.2. System dynamics

In order to describe the motion of the lander it is necessary to define a suitable coordinate system in moon centered inertial frame XYZ as shown in Fig. 2a and formulate equations of motion in accordance with physical laws governing the system. Considering the vehicle as a point mass within the Moon's gravity field, the three dimensional equations of motion with rotational velocity of moon is given by

Please cite this article in press as: Mathavaraj, S., et al. Constrained optimal multi-phase lunar landing trajectory with minimum fuel consumption. Adv. Space Res. (2017), https://doi.org/10.1016/j.asr.2017.09.016

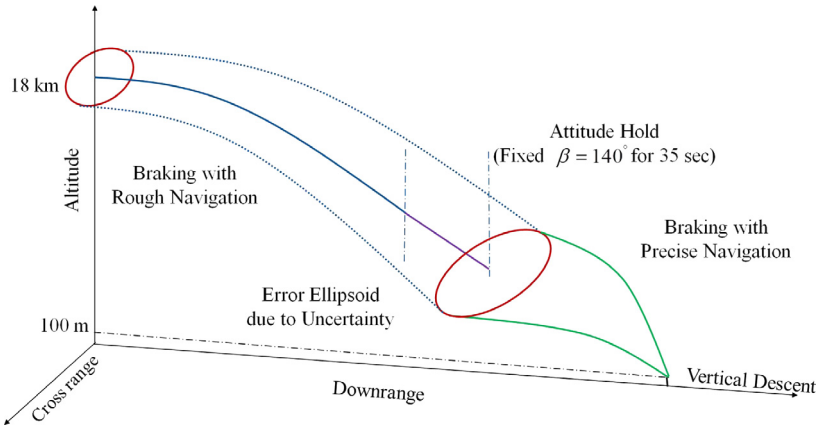

Fig. 1. Powered descent phase mission scenario.

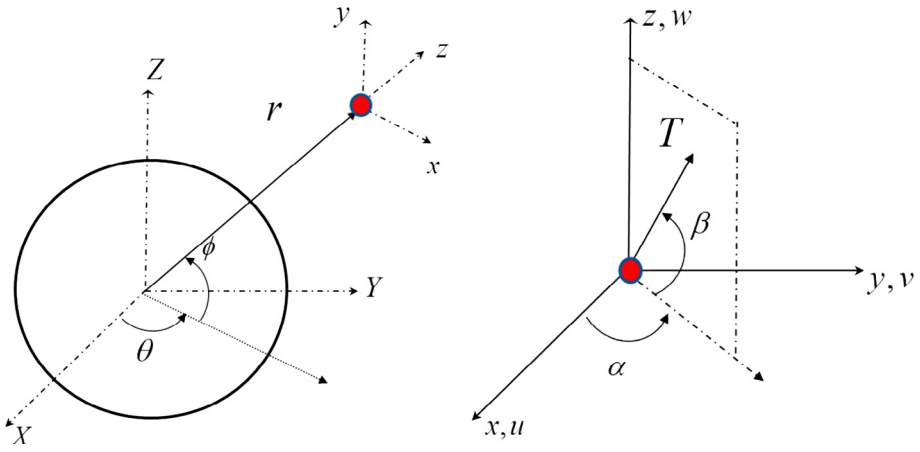

(a) Spacecraft orbiting around the moon (b) Thrust vector in body frame

Fig. 2. Co-ordinate frames.

$$
\begin{aligned}
\dot{r} &= w \\
\dot{\theta} &= \frac{u}{r\cos\phi} \\
\dot{\phi} &= \frac{v}{r} \\
\dot{w} &= \frac{T\sin\beta}{m} - \frac{\mu}{r^2} + \frac{(u^2+v^2)}{r} + \left(-2u\omega\cos\phi + r\omega^2\cos^2\phi\right) \\
\dot{u} &= \frac{(T\cos\alpha\cos\beta)}{m} + \frac{(-uw + uv\tan\phi)}{r} \\
&\quad + (-2w\omega\cos\phi + 2v\omega\sin\phi) \\
\dot{v} &= \frac{(T\sin\alpha\cos\beta)}{m} + \frac{(-vw - u^2\tan\phi)}{r} \\
&\quad + \left(-2u\omega\sin\phi - r\omega^2\sin\phi\cos\phi\right) \\
\dot{m} &= -\frac{T}{I_{sp}g}
\end{aligned}
\tag{1}
$$

In Eq. (1), r represents the radial distance from the center of the moon and θ, ϕ represents the longitude and latitude traced by the lander, respectively. u, v, w represents the tangential velocity, across velocity and vertical velocity components, respectively and m represents the instantaneous mass of the lander. Also μ is the moon's gravitational constant and I_{sp} is specific impulse of the engine considered for simulation. The control parameters considered are thrust T, thrust vector declination angle β and thrust vector right ascension angle α in body frame xyz is shown in Fig. 2b. For further details one can refer to Vinh et al. (1980).

For the optimization algorithm, normalization is required for numerical conditioning of the variables. So, using basic variables like lander's initial distance (r_i) from the center of moon, radius of the moon (r_m) and lander's initial mass (m_i), normalizing variables are chosen as given below:

$$
\begin{aligned}
V_n &= \left|\sqrt{\mu/r_i}\right| \\
d_n &= |r_m| \\
m_n &= |m_i|
\end{aligned}
$$

Please cite this article in press as: Mathavaraj, S., et al. Constrained optimal multi-phase lunar landing trajectory with minimum fuel consumption. Adv. Space Res. (2017), https://doi.org/10.1016/j.asr.2017.09.016

2.3. System dynamics as algebraic constraints

The dynamical equation constraint in each phase is formulated into non-linear programming constraints as explained in Appendix A

$$\begin{aligned}
&\sum_{l=0}^{N} D_{kl} r(\tau_l) - \frac{(t_f - t_i)}{2} w|_{\tau_k} = 0 \\
&\sum_{l=0}^{N} D_{kl} \theta(t_l) - \frac{(t_f - t_i)}{2} \frac{u}{r\cos\phi}\Big|_{\tau_k} = 0 \\
&\sum_{l=0}^{N} D_{kl} \phi(\tau_l) - \frac{(t_f - t_i)}{2} \frac{v}{r}\Big|_{\tau_k} = 0 \\
&\sum_{l=0}^{N} D_{kl} w(\tau_l) - \frac{(\tau_f - \tau_i)}{2} \left(\begin{array}{l} \frac{T\sin\beta}{m} - \frac{\mu}{r^2} + \frac{(u^2+v^2)}{r} \\ +\left(-2u\omega\cos\phi + r\omega^2\cos^2\phi\right) \end{array} \right)\Big|_{\tau_k} = 0 \\
&\sum_{l=0}^{N} D_{kl} u(\tau_l) - \frac{(t_f - t_i)}{2} \left[\begin{array}{l} \frac{(T\cos\alpha\cos\beta)}{m} + \frac{(-uw + uv\tan\phi)}{r} \\ +\left(-2w\omega\cos\phi + 2v\omega\sin\phi\right) \end{array} \right]\Big|_{\tau_k} = 0 \\
&\sum_{l=0}^{N} D_{kl} v(\tau_l) - \frac{(t_f - t_i)}{2} \left[\begin{array}{l} \frac{(T\sin\alpha\cos\beta)}{m} + \frac{\left(-vw - u^2\tan\phi\right)}{r} \\ +\left(-2u\omega\sin\phi - r\omega^2\sin\phi\cos\phi\right) \end{array} \right]\Big|_{\tau_k} = 0 \\
&\sum_{l=0}^{N} D_{kl} m(\tau_l) - \frac{(t_f - t_i)}{2} \left(\frac{T}{I_{sp} g_e} \right)\Big|_{\tau_k} = 0 \\
&k = 0, \ldots, N
\end{aligned} \tag{2}$$

2.4. Cost function selection

As discussed earlier, the spacecraft fuel consumption is to be minimized if it is to carry a enhanced payload mass for useful lunar explorations. So the cost function (J) for the optimal control problem is selected as minimization of acceleration.

$$J = \int_{t_0}^{t_f} T/m \quad dt \tag{3}$$

2.5. Path terminal constraints

As the trajectory is segmented into a multi-phase trajectory, there are several path constraints that are to be satisfied at initial/terminal condition of the segments. Fig. 1 provides the segmentation and mission scenario of the trajectory design.

2.5.1. Braking with rough navigation

This phase starts from the terminal conditions of the coasting phase. The objective of this phase is to decrease the orbital velocity and to ensure terminal conditions with appropriate altitude and attitude for camera imaging. Camera imaging capability determines the terminal altitude of this phase. Since image resolution improves as altitude decreases, ground test specifies an altitude upper limit below which image clarity is better for identifying a safe landing site. Also, the lander's terminal attitude of this phase is specified based on the mounting angle of the lander camera and its field of view.

$$\begin{aligned}
&\left[r_1(t_{1i}) - r_{1s_i} \quad w_1(t_{1i}) - w_{1s_i} \quad u_1(t_{1i}) - u_{1s_i} \quad v_1(t_{1i}) - v_{1s_i}\right]^T = 0 \\
&\left[r_1(t_{1f}) - r_{1s_f} \quad \beta_1(t_{1f}) - \beta_{1s_f} \quad \alpha_1(t_{1f}) - \alpha_{1s_f}\right]^T = 0 \\
&\left[w_1(t_{1f}) - w_{1s_f} \quad u_1(t_{1f}) - u_{1s_f} \quad v_1(t_{1f}) - v_{1s_f}\right]^T < 0
\end{aligned} \tag{4}$$

In Eq. (4) first two equation enforces the difference in initial $(r_1(t_{1i}), w_1(t_{1i}), u_1(t_{1i}), v_1(t_{1i}))$ and final $(r_{1s_f}, \beta_{1s_f}, \alpha_{1s_f})$, states and controls to zero with respect to desired nominal condition $(r_{1s_i}, w_{1s_i}, u_{1s_i}, v_{1s_i}, r_{1s_f}, \beta_{1s_f}, \alpha_{1s_f})$. The last equation enforces that the terminal velocity achieved should be less than the velocity sensor maximum capability $(w_{1s_f}, u_{1s_f}, v_{1s_f})$.

2.5.2. Attitude hold

The objective in this phase is to image the selected portion of the lunar surface, process it for the current location information so that in subsequent phase the guidance command guides the lander to the targeted safe landing site. The 'braking with rough navigation phase' specifies the initial conditions of this phase. It is to be noted that, at the terminal condition of 'braking with rough navigation phase', the lander is forced into a favorable orientation for imaging by the camera. Throughout this phase, the thrust firing and attitude are held constant to avoid chattering during image capturing through the following constraints.

$$\left[T_2(t) - T_1(t_{1f})\beta_2(t) - \beta_1(t_{1f})\alpha_2(t) - \alpha_1(t_{1f})\right]^T = 0 \tag{5}$$

Here, the thrust vector throughout this phase $T_2(t), \beta_2(t), \alpha_2(t)$ remains same as the phase 1 terminal thrust vector $T_{1s_f}, \beta_{1s_f}, \alpha_{1s_f}$ so that continuity of the control vector is enforced as constraints.

2.5.3. Braking with precise navigation

At the terminal part of the 'attitude hold phase', the correct update of the position of the lander with respect to safe site is known. The objective of the 'braking with precise navigation' is to guide the lander from the terminal condition of the 'attitude hold phase' to an altitude of 100 m above the landing site with zero kinetic energy. Further, in the terminal condition, the lander's orientation should be vertical, which favors the lander's leg to touch the moon's surface satisfying the constraints given below.

$$\begin{aligned}
&\left[r_3(t_{3f}) - r_{3s} \quad \theta_3(t_{3f}) - \theta_{3s} \quad \phi_3(t_{3f}) - \phi_{3s}\right]^T = 0 \\
&\left[u_3(t_{3f}) - u_{3s} \quad v_3(t_{3f}) - v_{3s} \quad w_3(t_{3f}) - w_{3s}\right]^T = 0 \\
&\left[\beta_3(t_{3f}) - \beta_{3s} \quad \alpha_3(t_{3f}) - \alpha_{3s}\right]^T = 0
\end{aligned} \tag{6}$$

Here, the final latitude and longitude constraint enforces the difference between the phase 3 final position $\theta_3(t_{3f})$, $\phi_3(t_{3f})$ and identified safe site position θ_{3s}, ϕ_{3s} as zero i.e. the lander's terminal position is above the safe site.

Please cite this article in press as: Mathavaraj, S., et al. Constrained optimal multi-phase lunar landing trajectory with minimum fuel consumption. Adv. Space Res. (2017), https://doi.org/10.1016/j.asr.2017.09.016

3. Results from simulation experiments

Extensive simulation experiments have been carried out for solving Multi-phase lunar landing problem explained in the earlier sections. The algorithm uses the suite of mathematical nonlinear programming DIDO solvers in MATLAB (Ross, 2007). The solver uses sequential quadratic programming which solves a sequence of subproblems based on the quadratic model of the original problem (Ross and Fahroo, 2004). The Lagrangian is constructed using the quadratic model with linear and non-linear constraints using Karush-Kuhn-Tucker necessary condition. The idea behind this approach is to model at the current iterated solution by quadratic programming subproblem, then use the minimizer of this subproblem to define a next iterated solution. The step size at every iteration is based on the lagrangian merit function with a linesearch method (Nocedal and Wright, 2006). The difference between the current and previous iterated solution is checked for the tolerance specified. If the difference is less than the tolerances, the iteration stops otherwise the search continues in the descent direction calculated by sequential quadratic programming. The covector mapping principle eliminates the curse of sensitivity associated with solving costates of the optimal control problem. The optimality of the generated spectrally accurate solution is verified by Pontryagin's Minimum Principle.

Here, the problem is formulated as detailed in Section 2 which consists of a set of equality and non-equality bounds. Normalization is performed so that the algorithm searches for feasible solution in the same non-dimensional domain as discussed above.

For the analysis, the state and control guess history for each phase is simulated using the explicit analytical guidance solution derived from the linearized dynamics. Here the minimization of jerk is taken as cost function to obtain a new optimal guidance law using calculus of variation approach. Note the algorithm not only enforces the final position and velocity but also acceleration at final time. This gives the flexibility to ensure the desired thrust angle orientation at the terminal condition of each phase. In explicit guidance scheme, the final time is derived from the sixth order time-to-go polynomial which is a function of states (Mathavaraj and Padhi, 2017).

However, the optimum control profile from the solver is used to propagate the system dynamics with suitable time step by Runge-Kutta fourth order method for validating the trajectory. In order to study the additional fuel requirement due to orbit determination error as well as maneuver error, the error ellipse by Monte-carlo simulation is also carried out using dispersed initial conditions.

3.1. Optimal control solution for nominal case

Initial and final condition for the lander is provided in Table 1. Table 2 gives the parameters used for the optimal control problem simulation. In the formulation, these conditions are absorbed as constraints in the optimal control algorithm. As seen in Table 1, each phase has its own mission constraints. Phase 1 ('braking with rough navigation') terminal condition in altitude and attitude has been selected based on camera sensor as explained in Section 2.5.1. Phase 2 ('attitude hold') constraint emphasizes on avoiding chattering during imaging. Phase 3 ('braking with precise navigation') constraints enforce soft vertical landing on desired site. Detailed description of these constraints has been discussed in Section 2. Four main 800 N engine is mounted diagonally opposite manner which provides total thrust of 3200 N. In phase 1 all four engines are ON to meet the thrust requirement and in phase 2, 3 two diagonally opposite thruster are switched OFF since lander's mass reduces due to fuel consumption in phase 1 in turn result in thruster requirement reduction in phase 2, 3. Table 3 provides the details of the thrust control constraint in each one of the phases and should be suitably handled in the trajectory as a constraint.

Table 1
Terminal Condition (T.C.) for multi-phase landing problem.

Phase	Variables	Initial	Final
1	Vertical velocity (v_{1s})	0	Free
	Tangential velocity (u_{1s})	1.69 km/s	Free
	Across velocity (w_{1s})	0 km/s	Free
	Altitude ($r_{1s} - r_m$)	18.2 km	7 km
	Thrust right ascension angle (α_{1s})	Free	0 deg
	Thrust declination angle (β_{1s})	Free	140 deg
2	Vertical velocity (v_{2s})	Phase 1 T.C.	Free
	Tangential velocity (u_{2s})	Phase 1 T.C.	Free
	Across velocity (w_{2s})	Phase 1 T.C.	Free
	Altitude ($r_{2s} - r_m$)	Phase 1 T.C.	Free
	Thrust (T_{2s})	Phase 1 T.C. $\forall t$	
	Thrust right ascension angle (α_{2s})	0 deg $\forall t$	
	Thrust declination angle (β_{2s})	140 deg $\forall t$	
3	Vertical velocity (v_{3s})	Phase 2 T.C.	0
	Tangential velocity (u_{3s})	Phase 2 T.C.	0
	Across velocity (w_{3s})	Phase 2 T.C.	0
	Altitude ($r_{3s} - r_m$)	Phase 2 T.C.	100 m
	Downrange ($r_m\theta_{3s}$)	Phase 2 T.C.	10000 m
	Crossrange ($r_m\phi_{3s}$)	Phase 2 T.C.	0 m
	Thrust right ascension angle (α_{3s})	Phase 2 T.C.	0 deg
	Thrust declination angle (β_{3s})	Phase 2 T.C.	90 deg

Table 2
Mission parameters for simulation.

Variables	Values
Gravity	1.62 m/s^2
Gravitational parameter	4902.779×10^9 km^3/s^2
Moon radius	1737.1 km
Specific impulse	320 s

Table 3
Thrust constraint for multi-phase landing problem.

Phase	Upper bound	Lower bound
1	100% of $800 \times 4\ N$	40% of $800 \times 4\ N$
2, 3	100% of $800 \times 2\ N$	40% of $800 \times 2\ N$

Please cite this article in press as: Mathavaraj, S., et al. Constrained optimal multi-phase lunar landing trajectory with minimum fuel consumption. Adv. Space Res. (2017), https://doi.org/10.1016/j.asr.2017.09.016

Fig. 3a shows the decreasing altitude profile of the lander satisfying all mission constraints i.e. first phase terminal constraint of 7 km and third phase terminal constraint of 100 m. Fig. 3a also shows the down range traced by the lander and Fig. 3b shows the cross range traced by the lander reaching desired landing site at final time. Fig. 3c-e shows the velocity components of the lander satisfying the mission constraints of soft landing. It is to be noted that terminal velocity attained at the 'braking with rough navigation phase' is optimal since it is not constrained in the formulation. To demonstrate this fact, simulation exercises have been carried out to compare fuel consumption with obtained optimal rough braking terminal states to non-optimal states.

Case 1 and case 2 are selected such that the total achieved velocity is more and less respectively than optimal

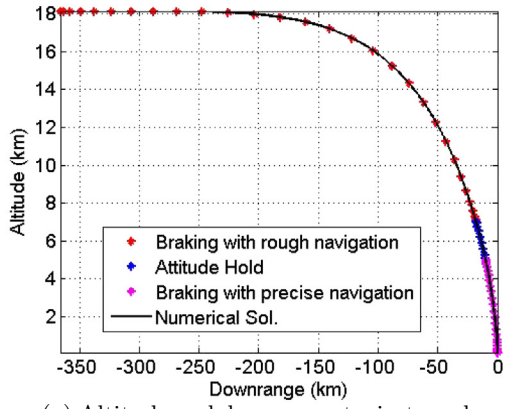

(a) Altitude and downrange trajectory during descent of the lander

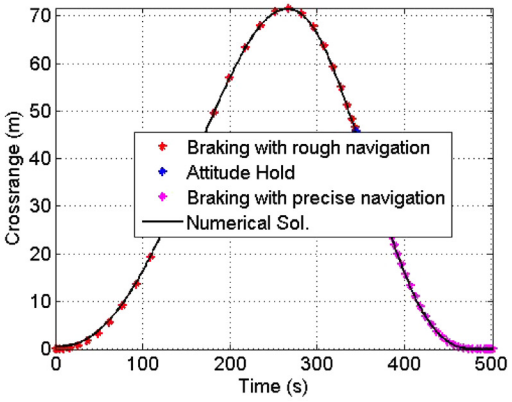

(b) Crossrange traced by the lander

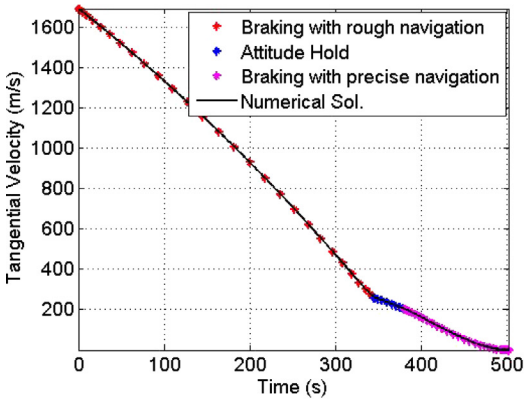

(c) Tangential velocity profile of the lander

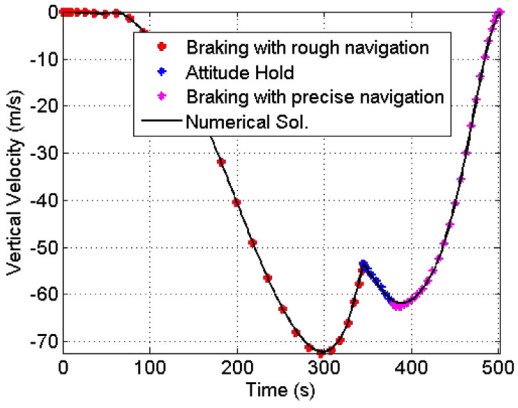

(d) Radial velocity profile of the lander

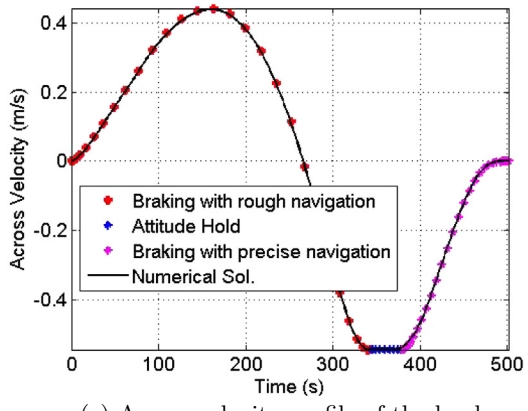

(e) Across velocity profile of the lander

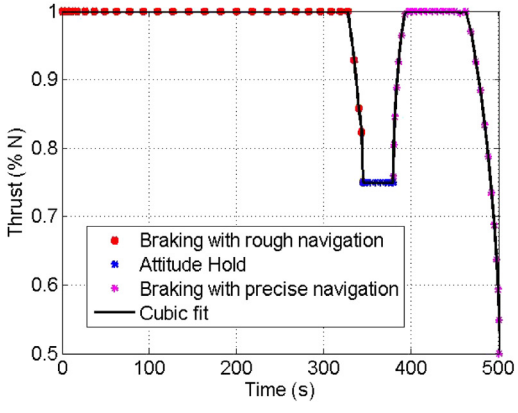

(f) Demanded thrust firing for achieving mission goals

Fig. 3. Nominal case solution.

Please cite this article in press as: Mathavaraj, S., et al. Constrained optimal multi-phase lunar landing trajectory with minimum fuel consumption. Adv. Space Res. (2017), https://doi.org/10.1016/j.asr.2017.09.016

Table 4
Braking with rough navigation phase terminal states.

Case study	Component	Velocity	Total propellant consumed
Optimal	Radial	−53 m/s	428.21 kg
	Along track	259 m/s	
	Across track	−0.5 m/s	
Case 1	Radial	−15 m/s	438.56 kg
	Along track	300 m/s	
	Across track	20 m/s	
Case 2	Radial	−55 m/s	432.89 kg
	Along track	230 m/s	
	Across track	−20 m/s	

values required to cover the desired downrange value. Table 4 shows the fuel savings of 10 kg if the states are free to take the optimum values that extremizes the performance index. The first simulation run depicts a case where the total velocity is more and the excess kinetic energy has to be reduced before reaching the landing site which demands more fuel consumption. On the other hand, the second simulation run depicts a case where the total velocity is low and the lander needs extra kinetic energy for traveling (extra propellant consumption) to reach the landing site. It is to be noted that the multi-phase problem can be solved either by considering each phase separately or by handling them together. When solving individually, the process becomes very laborious and tedious especially when many deboost initial conditions are to be studied. However, in the formulation presented in this study, the process is carried out with all three phases together which makes it elegant. Fig. 3f provides the demanded thrust throttling percentage after satisfying the mission constraints as given in Table 3. In Attitude hold phase, since the throttling percentage and orientation is held constant, the vertical velocity components increases as seen in Fig. 3d. In the subsequent braking with precise navigation phase, the throttling percentage and orientation is derived from the current states to achieve soft landing at landing site.

The thrust vector declination angle profile provided in Fig. 4a satisfying constraints viz attaining terminal constraint of 140 deg at the 'braking with rough navigation phase' and 90 deg at the 'braking with precise navigation phase' ensures the vertical landing over the desired site. Fig. 4b shows the thrust vector right ascension angle satisfying terminal constraints. Note that in 'attitude hold phase', the throttling percentage and thrust declination as well as right ascension angle is maintained constant throughout as per the design and which is demanded by Eq. (5).

In Legendre Pseudospectral method since all dynamic and terminal constraints are converted into either equality and or inequality constraints, the algorithm is capable of accounting additional constraints due to desired landing site as well. In the entire simulation, the total number of Legendre-Gauss-Lobatto points chosen are 70 out of which 30 each has been allocated for 'braking with rough navigation' and 'braking with precise navigation' phases and the remaining 10 is used for 'attitude hold phase'. Since the acceleration is held constant in 'attitude hold phase' the number of grid points is chosen less when compared to other phases (Ross and Fahroo, 2004). The numbers of grid points are sufficient since the control profile is used to propagate the system dynamics and the trajectory has been validated. Hence it is shown that using pseudospectral knots, multiphase lunar landing problem is solved efficiently satisfying all mission constraints with a single optimal control framework. Table 5 signifies the reduction of fuel consumption due to multiphase formulation when compared to explicit guidance (Mathavaraj and Padhi, 2017) for soft landing at desired site.

3.2. Study on effect of error dispersions

In this design, from 'deboost phase' to the end of 'rough braking navigation phase', the navigation process is planned to rely on inertial navigation system totally. The other main parameters for control such as absolute altitude

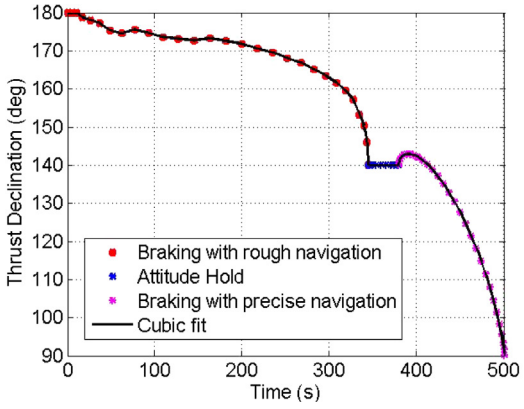

(a) Thrust Declination Angle profile ensuring vertical landing of lander

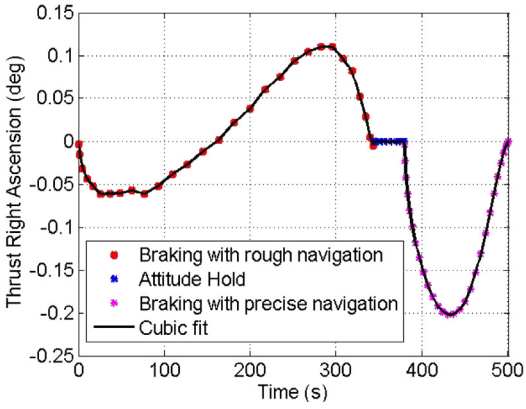

(b) Thrust Right Ascension Angle profile ensuring vertical landing of lander

Fig. 4. Nominal case solution.

Please cite this article in press as: Mathavaraj, S., et al. Constrained optimal multi-phase lunar landing trajectory with minimum fuel consumption. Adv. Space Res. (2017), https://doi.org/10.1016/j.asr.2017.09.016

Table 5
Comparison with explicit guidance.

Case study	Initial position	Values	Propellant consumed
Legendre Pseudospectral	Altitude	18 km	430.91 kg
	Downrange	−389 km	
	Cross range	−600 m	
Explicit	Altitude	18 km	454.66 kg
	Downrange	−389 km	
	Cross range	−600 m	

from laser altimeter, position reference from hazard detection camera and velocity components from velocity meter are obtained from sensors that are switched on only at the start of the 'attitude hold phase'. The sensors are so designed that they can perform efficiently only in this altitude range. At the end of 35 s period (or start of 'precision braking navigation phase'), it is expected that the absolute value of position, altitude and velocity can be estimated by the onboard process. The error estimates and the capability of the algorithm to counter the error for precision landing are explained in the following. When deboost of the landercraft from the 100 km circular parking orbit is initiated, it is effected based on the Orbit Determination (OD) results for that parking orbit. The errors of OD estimation along with other factors such as maneuver performance and misalignment of thrusters have a considerable influence on the precision of descent trajectory of the lander and therefore, a simulation study is conducted using Monte-Carlo procedure. Based on Chandrayaan-1 on-orbit experience, the OD estimation statistics are determined to be 1 km (3σ) in position and 20 cm/s (3σ) in velocity and for a 100 km circular parking orbit. The corresponding 3σ errors in radial, along and across track directions is provided in Table 6. Using the statistical values of Table 6, one hundred initial conditions of OD for 100 km parking orbit are randomly generated for deboost conditions and the deboost is carried out.

The de-boost orbit is selected as 100×18 km elliptical transfer orbit based on the mean Moon model and the expected landing site undulations. The deboost δV maneuver error is assumed to be 1% of total thrust magnitude 4×800 N and about 0.1 deg in thrust direction. A one thousand different sets of state vectors accounting for thrust and alignment errors are generated from the one hundred initial conditions generated earlier. The trajectory is propagated for the nominal coasting duration in transfer orbit phase to reach 18 km perilune position and the resulting deviations in altitude, down and cross ranges from such initial state vectors are generated. When these initial conditions are used in open loop simulation during 'rough braking navigation phase', the terminal errors at the end of 'attitude hold phase' are accumulated to be 2 km in altitude, 4 km in downrange and the 0.1 km in cross range. The statistical details are provided in Table 6.

3.3. Regeneration of braking with precise navigation phase

At the end of the 'attitude hold phase', due to the estimation process onboard for altitude, position and velocity, there is a fairly good estimate of the errors in the initial conditions available for correction. Using these initial conditions and knowing the final landing site details, the optimal trajectory are recomputed using Legendre pseudo spectral method for all one thousand cases and all states of the simulation are plotted in Fig. 5. Fig. 5a provides the dispersions of altitude, downrange and crossrange arising due to various error sources considered above. It is to be noted that the error sources considered have a significant effect on the final absolute velocity of the lander. Fig. 5b portrays that in spite of all the velocity error noted in such cases, the re-computation of the trajectory is enacted accurately such that the final velocity is almost zero for all cases satisfying soft landing mission constraint but at the cost of some extra fuel spending. However, based on the initial position and velocity with respect to the landing site, the acceleration demand on the lander to reach the landing site is found to vary. Table 7 provides the additional fuel requirement due to dispersion in the states but managed the fuel expenditure within the fuel margin.

Fig. 5c and d gives the percentage of the thrust demanded and fuel mass consumption for all the cases considered. Note that the demanded thrust requirement is within the main engine capability of the lander of

Table 6
Orbit determination error.

Phase (Altitude)	Component	Position	Velocity
De-orbit (100 km)	Radial	400 m	6 cm/s
	Along track	900 m	18 cm/s
	Across track	10 m	2 cm/s
Braking with rough navigation (18 km)	Radial	0.5 km	3 m/s
	Along track	3 km	0.3 m/s
	Across track	0.05 km	0.09 m/s
Braking with precise navigation (5.5 km)	Radial	2 km	4 m/s
	Along track	4 km	1 m/s
	Across track	0.1 km	0.2 m/s

Please cite this article in press as: Mathavaraj, S., et al. Constrained optimal multi-phase lunar landing trajectory with minimum fuel consumption. Adv. Space Res. (2017), https://doi.org/10.1016/j.asr.2017.09.016

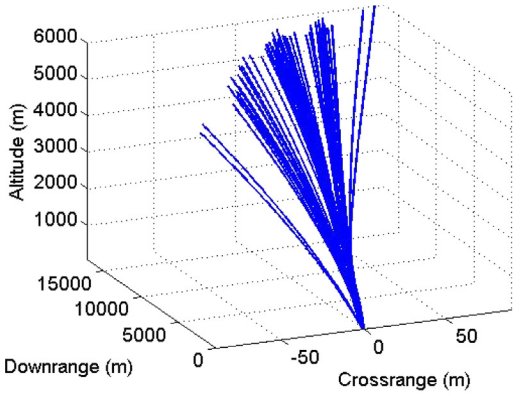

(a) Three dimensional positional correction of the lander

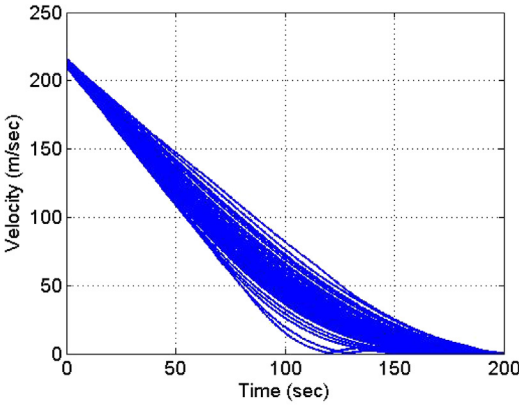

(b) Total velocity correction of the lander

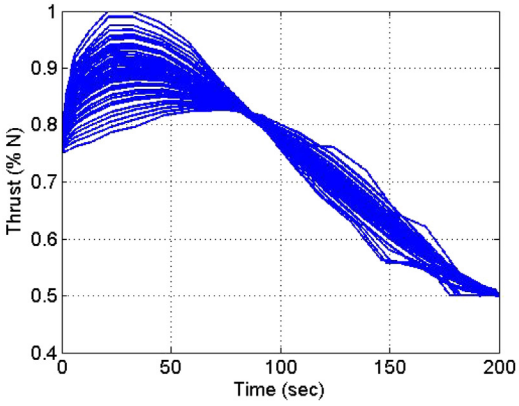

(c) Thrust requirement for the the lander

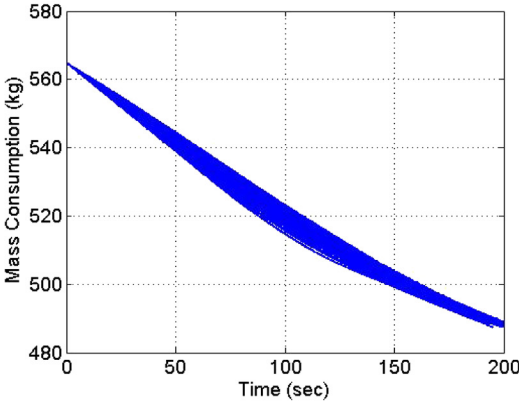

(d) Mass consumption of the lander

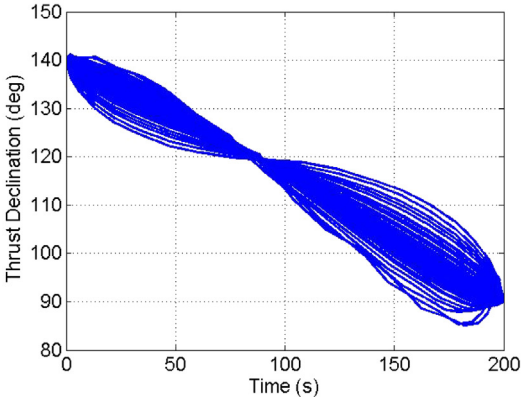

(e) Thrust declination angle of the lander

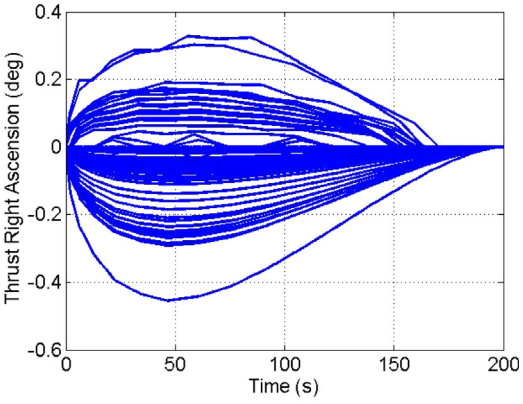

(f) Thrust right ascension angle of the lander

Fig. 5. Regeneration of braking with precise navigation phase.

2×800 N. Fig. 5e shows the demanded thrust vector declination angle profile whose initial condition is same as 'attitude hold phase' angle 140 deg satisfying the continuity at the transition from 'attitude hold phase' to 'braking with precise navigation phase'. The terminal condition of the thrust declination angle is 90 deg for all error cases ensuring vertical orientation at the final time. Fig. 5f shows the thrust vector right ascension angle profile demanding the corrective out of plane maneuvers wherever the crossrange error has to be nullified. It is to be noted that at the final time, the thrust vector right ascension angle is 0 deg which favors the lander's leg orientation for vertical touchdown.

Please cite this article in press as: Mathavaraj, S., et al. Constrained optimal multi-phase lunar landing trajectory with minimum fuel consumption. Adv. Space Res. (2017), https://doi.org/10.1016/j.asr.2017.09.016

Table 7
Fuel consumption in braking with precise navigation phase.

Case	Error component	Position	Fuel consumption
Nominal	Radial	400 m	60.47 kg
	Along track	900 m	
	Across track	10 m	
Case 1	Radial	2 km	65.35 kg
	Along track	4 km	
	Across track	0.1 km	
Case 2	Radial	−2 km	68.58 kg
	Along track	−4 km	
	Across track	−0.1 km	

4. Conclusion

A unified multi-phase constrained optimal trajectory problem is posed and solved to optimally guide a lander from the perilune of the transfer orbit to a desired altitude for smooth vertical descent in order to achieve soft-landing on the surface of the moon. This design accounts for various operational constraints and suitably segments the trajectory into three phases namely, the 'braking with rough navigation phase', 'attitude hold phase' and 'braking with precise navigation phase' of the landing sequence. All relevant mission constraints such as upper and lower bounds of the thrusters, attitude hold constraint to cater for the look angle constraint of the downward looking vision camera and time required for image processing have been considered in the optimal control problem formulation. During the cases of high terminal error due to dispersions, the 'precision navigation terminal phase' guidance history is regenerated and the additional fuel requirement is revealed. The proposed approach also leads to a minimum fuel consumption solution, which is an important objective of this study. Extensive simulation studies show that following the strategy proposed in this paper the desired terminal position, velocity and attitude are achieved. In addition, proper orientation and safe soft landing is ensured over the desired landing site. It is also shown that the dispersions due to orbit determination and maneuver are absorbed and a precise landing can be achieved.

Acknowledgment

The authors are thankful to the Indian Space Research Organisation (ISRO) for giving an opportunity to work on this challenging problem. The authors are also thankful to the Dept. of Science and Technology, Govt. of India, for its financial support through the FIST grant in acquiring the necessary infrastructure at the Indian Institute of Science, Bangalore, to carry out this research successfully.

Appendix A. Legendre pseudospectral method: a brief summary

Even though the Legendre pseudo-spectral method has evolved as a popular technique and is used by many researchers across the globe, the theoretical details of the method is not found in most of the literature to the best of the knowledge of the authors. Hence an attempt has been made here to explain the technique in a lucid manner so as to make the technique accessible and understandable to large practicing engineering researchers and to inform what precautions one must adhere to operating successfully while solving practical problems.

A.1. Problem objective

A generalized optimal control setup is with the objective to minimize the cost function J in Eq. (A.1)

$$J = \varphi\left(X\left(t_f\right), t_f\right) + \int_{t_0}^{t_f} L(X(t), U(t), t)dt \tag{A.1}$$

subjected to the following dynamical constraints in Eq. (A.2) and trajectory constraints Eqs. (A.3), (A.4)

$$\dot{\mathrm{X}}(t) = f(\mathrm{X}(t), \mathrm{U}(t)) \tag{A.2}$$

$$e(\mathrm{X}(t_0), \mathrm{X}(t_f)) = 0 \tag{A.3}$$

$$h(\mathrm{X}(t), \mathrm{U}(t)) \leqslant 0 \tag{A.4}$$

where t_0, t_f represents the initial and final time, X represents the state vector, U represents the control vector, $\varphi\left(X\left(t_f\right), t_f\right)$ represents the terminal cost term, $L(X, U, t)$ represents the integral cost term, $h(\mathrm{X}, \mathrm{U}), e(\mathrm{X}(t_0)\mathrm{X}(t_f))$ represent the path and terminal constraints, respectively.

A.2. Discretization of the system dynamics

Usually collocation methods use piecewise-continuous functions to approximate the state and control variables at the arbitrary subintervals. However, the Legendre pseudo-spectral method uses globally interpolating Lagrange polynomials as trial functions to approximate the state and control variables at the nodes, which are called Legendre-Gauss-Lobatto (LGL) points.

A.2.1. Selection of grid points

The time interval $(t_f - t_i)$ can be transformed to τ domain by change of variables

$$\tau \rightarrow -1 + 2(t - t_i)/\left(t_f - t_i\right) \tag{A.5}$$

This transformation from the real time domain to the τ domain is required because the LGL points are defined between $[-1\,1]$. So the $N+1$ points are $\tau_l\ l = 0, \ldots, N$ which specifies $\tau_0 = -1, \tau_N = 1$ and other LGL points are the zeros of the derivative of the Legendre polynomial of degree $N, (L_N)$.

A.2.2. State dynamics approximation

As stated earlier, approximating the state $X(t)$ and control $U(t)$ trajectory by N^{th} degree Legendre polynomial leads to

Please cite this article in press as: Mathavaraj, S., et al. Constrained optimal multi-phase lunar landing trajectory with minimum fuel consumption. Adv. Space Res. (2017), https://doi.org/10.1016/j.asr.2017.09.016

$$X(\tau) \approx X^N(\tau) = \sum_{l=0}^{N} X(\tau_l)\rho_l(\tau)$$
$$U(\tau) \approx U^N(\tau) = \sum_{l=0}^{N} U(\tau_l)\rho_l(\tau) \quad (A.6)$$

where, Lagrange polynomials $\rho_l(\tau)$ in τ domain is given by

$$\rho_l(\tau) = \frac{g(\tau)}{(\tau-\tau_l)\dot{g}(\tau_l)} \quad (A.7)$$

where $g(\tau)$ define the LGL grid points and it's corresponding derivative is $\dot{g}(\tau)$

$$g(\tau) = (1-\tau^2)\dot{L}_N(\tau)$$
$$\dot{g}(\tau) = -N(N+1)L_N(\tau) \quad (A.8)$$

Eq. (A.6) represents polynomials of N^{th} order, which is used to interpolate the functions at the LGL points. Substituting Eq. (A.8) in Eq. (A.7) and simplifying provides

$$\rho_l(\tau) = -\frac{1}{N(N+1)L_N(\tau_l)} \times \frac{(1-\tau^2)\dot{L}_N(\tau)}{\tau-\tau_l} \quad (A.9)$$
$$\rho_l(\tau) = \begin{cases} 1 & if \quad l = k \\ 0 & if \quad l \neq k \end{cases}$$

Differentiating Eq. (A.6) once and substituting in Eq. (A.2) provides

$$\dot{X}(\tau_k) = \sum_{l=0}^{N} X(\tau_l)\dot{\rho}_l(\tau_k) \quad (A.10)$$

$$\dot{\rho}_l(\tau) = \frac{d}{d\tau}\left[-\frac{1}{N(N+1)L_N(\tau_l)} \times \frac{(1-\tau^2)\dot{L}_N(\tau)}{\tau-\tau_l}\right] \quad (A.11)$$

For $\tau = \tau_k; k \neq l$ Eq. (A.11) is rewritten as

$$\dot{\rho}_l(\tau) = \frac{L_N(\tau_k)}{L_N(\tau_l)(\tau_k-\tau_l)} \quad (A.12)$$

For $\tau = \tau_k; k = l$ results in an indeterminate form. Using L'Hopital's rule and carrying out necessary substitutions result in

$$\dot{\rho}_l(\tau) = \frac{L_N{}'(\tau)}{2L_N(\tau_l)} \quad (A.13)$$

Case $\tau = \tau_k; \quad k = l \neq 0, N; \quad \dot{\rho}_l(\tau_k) = 0$
Case $\tau = \tau_k; \quad k = l = 0; \quad \dot{\rho}_l(\tau_k) = -\frac{N(N+1)}{4}$
Case $\tau = \tau_k; \quad k = l = N; \quad \dot{\rho}_l(\tau_k) = \frac{N(N+1)}{4}$

The differentiation matrix $D_{kl} = \dot{\rho}_l(\tau_k)$ in Eq. (A.14) is an $(N+1)\times(N+1)$ matrix after the discretization of the right-hand side of the state equation.

$$D = [D_{kl}] = \begin{cases} \frac{L_N(\tau_k)}{L_N(\tau_l)(\tau_k-\tau_l)} & k \neq l \\ -\frac{N(N+1)}{4} & k = l = 0 \\ \frac{N(N+1)}{4} & k = l = N \\ 0 & otherwise \end{cases} \quad (A.14)$$

A.3. Discretization of the cost function

The idea is to convert the integral term in the cost function into an algebraic constraints using Gauss-Lobatto integration rule. Using Eq. (A.6) in Eq. (A.1) and after simplifying one obtains

$$J^N = \varphi\left(X^N, \tau_N\right) + \frac{(\tau_f-\tau_0)}{2}\sum_{k=0}^{N} L^k(X(\tau_k), U(\tau_k), \tau_k)\int_{-1}^{1}[\rho_l(\tau)]d\tau \quad (A.15)$$

Let the weight factor be

$$w_k = \int_{-1}^{1}\rho_l(\tau)d\tau = \frac{1}{g'(\tau_l)}\int_{-1}^{1}\left(\frac{g(\tau)}{(\tau-\tau_l)}\right)d\tau \quad (A.16)$$

In order to evaluate w_k, consider Christoffel Darboux Identity as given below.

$$B_m(\tau,z) = \sum_{k=0}^{m}\left[\frac{L_k(\tau)L_k(z)}{\gamma_k}\right] = \left[\frac{(L_{m+1}(\tau)L_m(z) - L_m(\tau)L_{m+1}(z))}{(A_{m+1}\gamma_m(\tau-z)/A_m)}\right] \quad (A.17)$$

Evaluate Eq. (A.17) for $N, N-1$ degree polynomials and using Eq. (A.7) in Eq. (A.17) results in

$$B_N(\tau,z) + \frac{N+1}{N}B_{N-1}(\tau,z) = \frac{(2N+1)}{2N} \times \frac{(L_N(z)g(\tau) - L_N(\tau)g(z))}{(\tau-z)} \quad (A.18)$$

Substituting $z = t_k$ i.e. zeros of $g(\tau)$ in Eq. (A.18) and integrating the equation on both sides once results

$$\int_{-1}^{1}\left(B_N(\tau,\tau_k) + \frac{N+1}{N}B_{N-1}(\tau,\tau_k)\right)d\tau = \frac{(2N+1)}{2N} \times L_N(\tau_k)\int_{-1}^{1}\frac{g(\tau)}{(\tau-\tau_k)} \quad (A.19)$$

Evaluating right-hand side of Eq. (A.19) provides

$$= \frac{(2N+1)}{2N} \times L_N(\tau_k)g'(\tau_k)w_k = -\frac{(2N+1)(N+1)}{2} \times [L_N(\tau_k)]^2 w_k \quad (A.20)$$

Similarly, evaluating left-hand side of Eq. (A.19) results in

$$\int_{-1}^{1}\left(B_N(\tau,\tau_k) + \frac{N+1}{N}B_{N-1}(\tau,\tau_k)\right)d\tau = \int_{-1}^{1}B_N(\tau,\tau_k)d\tau + \frac{N+1}{N}\int_{-1}^{1}B_{N-1}(\tau,\tau_k)d\tau \quad (A.21)$$

Using the identities

$$[L_{k+1}(\tau) - L_{k-1}(\tau)]|_{-1}^{1}\Big|_{k>0} = 0$$

$$\int_{-1}^{\tau}(2N+1)L_N(\tau)=L_{N+1}(\tau)-L_{N-1}(\tau)$$

evaluating first part of Eq. (A.21) with Eqs. (A.7), (A.17) results in

$$\begin{aligned}\int_{-1}^{1}B_N(\tau,\tau_k)d\tau&=\frac{L_0(\tau_0)}{2}[-L_1(\tau)+L_{-1}(\tau)]|_{-1}^{1}\\&+\sum_{k=1}^{N}\frac{L_k(\tau_k)}{2}[-L_{k+1}(\tau)+L_{k-1}(\tau)]|_{-1}^{1}\\&=-1\end{aligned}\tag{A.22}$$

Next, evaluating Eq. (A.21) using Eq. (A.22) provides

$$\begin{aligned}&\int_{-1}^{1}B_N(\tau,z)d\tau+\left(\frac{N+1}{N}\right)\int_{-1}^{1}B_{N-1}(\tau,z)d\tau\\&=-\frac{(2N+1)}{N}\end{aligned}\tag{A.23}$$

Using Eqs. (A.20), (A.23) in Eq. (A.19) results

$$-\frac{(2N+1)(N+1)}{2}\times[L_N(\tau_k)]^2w_k=-\frac{(2N+1)}{N}$$

from which w_k is evaluated as

$$w_k=\frac{2}{N(N+1)[L_N(\tau_k)]^2}\tag{A.24}$$

So the optimal control problem represented by Eqs. (A.1)–(A.4) is approximated by the following nonlinear programming problem. The performance index is reformulated as

$$J^N=\varphi\left(X^N,\tau_N\right)+\frac{(t_f-t_0)}{2}\sum_{k=0}^{N}L^k(X(\tau_k),U(\tau_k),\tau_k)w_k$$

$$w_k=\frac{2}{N(N+1)}\frac{1}{[L_N(\tau_k)]^2}$$

the state equation as

$$\frac{(t_f-t_0)}{2}f(X(\tau_k),U(\tau_k),\tau_k)-C_k=0\tag{A.25}$$

and the constraint equations as

$$e(\mathrm{X}(\tau_0),\mathrm{X}(\tau_N))=0$$

$$h(\mathrm{X}(\tau_k),\mathrm{U}(\tau_k))\leqslant 0$$

Legendre Pseudospectral method is mathematically complex and the number of nodes used for simulation determines the dimensional complexity of the problem. In general, Legendre Pseudospectral method needs more nodes for accurate solution for a multi-phase problem. However, Legendre Pseudospectral knotting allows calculation of solutions efficiently even with fewer nodes, which reduces the computational time. Here, the entire time domain is divided into smaller subdomains where Legendre Pseudospectral knots is enforcing the continuity of the state and control variables in the transition regions. For more details refer to Ross and Fahroo (2004).

References

Afshari, H.H., Novinzadeh, A.B., Roshanian, J., 2009. An analytical guidance law of planetary landing mission by minimizing the control effort expenditure. J. Mech. Sci. Technol., 3239–3244

Banerjee, A., Padhi, R., 2015. Inverse polynomial based explicit guidance for lunar soft landing during powered braking. In: IEEE Conference on Control Applications, pp. 768–773. https://doi.org/10.1109/CCA.2015.7320710.

DSouza, C., 1997. An optimal guidance law for planetary landing. In: AIAA Guidance Navigation Control Conference, pp. 1376–1381. https://doi.org/10.2514/6.1997-3709.

Dunham, D., Farquhar, R., Eismont, N., Chumachenko, E., Aksenov, S., Genova, A., Horsewood, J., Furfaro, R., Kidd, J., 2013. Using lunar swingbys and libration-point orbits to extend human exploration to interplanetary destinations. In: 64th International Astronautical Congress, pp. 1932–1941.

Guo, Y., Hawkins, M., Wie, B., 2011. Optimal feedback guidance algorithms for planetary landing and asteroid intercept. In: AAS/AIAA Astrodynamics Specialist Conference, pp. 569–588.

Hawkins, A., Fill, T., Proulx, R., Feron, E., 2006. Constrained trajectory optimization for lunar landing. In: AAS Spaceflight Mechanics Meeting, pp. 06–153.

Hickman, J.M., Curtis, H., Landis, G., 1990. Design consideration for lunar based photovoltaic power systems. In: IEEE Photovoltaic Specialists Conference, pp. 1256–1262. https://doi.org/10.1109/PVSC.1990.111815.

Lee, A.Y., 2011. Optimal terminal descent guidance logic to achieve a soft lunar touchdown. In: AIAA Guidance Navigation Control Conference, pp. 8–11, http://hdl.handle.net/2014/41890.

Mathavaraj, S., Padhi, R., 2017. Explicit constrained terminal acceleration optimal guidance for three dimensional lunar landing. In: AIAA Guidance Navigation Control Conference, pp. 1267–1279. https://doi.org/10.2514/6.2017-1267.

Mathavaraj, S., Pandiyan, R., Ghatpande, N., Gopinath, N., 2012. A predictive guidance scheme for soft landing of a lunar module. In: 63rd International Astronautical Congress, pp. 1–12.

Mathavaraj, S., Pandiyan, R., Padhi, R., 2016. Optimal trajectory planning for multiphase lunar landing. In: Advances in Control and Optimization of Dynamical Systems, pp. 124–129.

McInnes, C.R., Radice, G., 1996. Line-of-sight guidance for descent to a minor solar system body. J. Guid. Control Dyn., 740–742 https://doi.org/10.2514/3.2169.

Nocedal, J., Wright, S.J., 2006. Sequential Quadratic Programming. Springer.

Park, B.G., Tahk, M.J., 2011. Three-dimensional trajectory optimization of soft lunar landings from the parking orbit with considerations of the landing site. Int. J. Control Autom. Syst., 1164–1172

Pieters, C., Goswami, J., Clark, R., Annadurai, M., Boardman, J., Buratti, B., Combe, J., Dyar, M., Green, R., 2009. Character and spatial distribution of OH/H_2O on the surface of the moon seen by M^3 on chandrayaan-1. Science, 568–572. https://doi.org/10.1126/science.1178658.

Ramkiran, B., Preethi, R., Rijesh, M., Kumar, G., Philip, N., Natarajan, P., 2016. Analytical optimal guidance algorithm for lunar soft landing with terminal control constraints. In: IEEE Indian Control Conference, pp. 481–486. https://doi.org/10.1109/INDIANCC.2016.744117.

Ross, I.M., 2007. A Beginners Guide to DIDO: A Matlab Application Package for Solving Optimal Control Problems. Elissar, TR-711, Technical Report.

Ross, I.M., Fahroo, F., 2004. Pseudospectral knotting methods for solving nonsmooth optimal control problems. J. Guid. Control Dyn., 397–405 https://doi.org/10.2514/1.342.

Ross, I.M., Karpenko, M., 2012. A review of pseudospectral optimal control: from theory to flight. In: Annual Reviews in Control, pp. 182–197. https://doi.org/10.1016/j.arcontrol.2012.09.002.

Please cite this article in press as: Mathavaraj, S., et al. Constrained optimal multi-phase lunar landing trajectory with minimum fuel consumption. Adv. Space Res. (2017), https://doi.org/10.1016/j.asr.2017.09.016

Sachan, K., Padhi, R., 2016. A near-optimal analytical guidance scheme for approach phase of autonomous lunar landing. In: IEEE Indian Control Conference, pp. 273–278. https://doi.org/10.1109/INDIANCC.2016.7441139.

Uchiyama, K., Shimada, Y., Ogawa, K., 2005. Minimum-jerk guidance for lunar lander. Trans. Jpn. Soc. Aeronaut. Space Sci., 34–39 https://doi.org/10.2322/tjsass.48.3.

Vinh, N.X., Busemann, A., Culp, R.D., 1980. Hypersonic and planetary entry flight mechanics. In: NASA-supported Research. University of Michigan Press, pp. 0–367.

Zhou, J., Teo, K.L., Zhou, D., Zhao, G., 2010. Optimal guidance for lunar module soft landing. In: Nonlinear Dynamics and Systems Theory, pp. 189–201.

Please cite this article in press as: Mathavaraj, S., et al. Constrained optimal multi-phase lunar landing trajectory with minimum fuel consumption. Adv. Space Res. (2017), https://doi.org/10.1016/j.asr.2017.09.016